Semi-flexible liquid crystalline polyesters based on twin di(*p*-oxybenzoyl) units X-ray study on smectic mesophase structures

Oriano Francescangeli[a]; Gianni Albertini[a]; Bin Yang[b]; Annino Sante Angeloni[c]; Michele Laus[c]; Emo Chiellini[d]; Giancarlo Galli[d]

[a] Dipartimento di Scienze dei Materiali e della Terra, Università di Ancona, Ancona, Italy [b] Istituto di Scienze Fisiche, Università di Ancona, Ancona, Italy [c] Dipartimento di Chimica Industrial e dei Materiali, Università di Bologna, Bologna, Italy [d] Dipartimento di Chimica e Chimica Industriale, Università di Pisa, Pisa, Italy

PLEASE SCROLL DOWN FOR ARTICLE

Semi-flexible liquid crystalline polyesters based on twin di(*p*-oxybenzoyl) units

X-ray study on smectic mesophase structures

by ORIANO FRANCESCANGELI and GIANNI ALBERTINI

Dipartimento di Scienze dei Materiali e della Terra,
Università di Ancona, Via Brecce Bianche, 60131 Ancona, Italy

and BIN YANG

Istituto di Scienze Fisiche, Università di Ancona,
Via Ranieri 65, 60131 Ancona, Italy

and ANNINO SANTE ANGELONI and MICHELE LAUS

Dipartimento di Chimica Industriale e dei Materiali,
Università di Bologna, Viale Risorgimento 4, 40136 Bologna, Italy
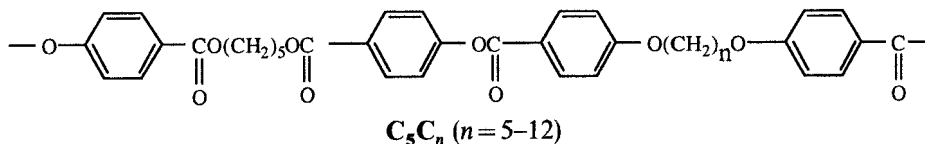
and EMO CHIELLINI* and GIANCARLO GALLI

Dipartimento di Chimica e Chimica Industriale, Università di Pisa,
Via Risorgimento 35, 56100 Pisa, Italy

An X-ray study is performed of oriented smectic mesophases of several polyesters consisting of two *p*-oxybenzoyl diads interconnected by a pentamethylene segment and a polymethylene segment of variable length. The X-ray diffraction patterns are very similar for all the samples and are constituted by one or more inner reflections, lying on the meridional line, and by two broad outer haloes split into two intense portions symmetrically placed above and below the equatorial line. The former reflections are attributed to the regular piling of the smectic layers; the latter are associated with the presence of rigid mesogenic groups that are tilted with respect to the layer normal, while the average chain axis lies perpendicular to the layer planes. Accordingly, the analysed smectic mesophases can be classified as unconventional smectic C. A structural model is proposed to account for the intensity profile of the X-ray patterns.

1. Introduction

In recent papers [1, 2] we have described the preparation and liquid crystalline mesomorphism of a new series of semi-flexible polyesters constituted by two mesogenic *p*-oxybenzoyl diads and two linear aliphatic chains sequenced in a regularly alternating fashion. The repeating unit of these polyesters is represented as follows:

$$-O-\langle\!\!\langle\bigcirc\rangle\!\!\rangle-\underset{\underset{O}{\|}}{C}O(CH_2)_5O\underset{\underset{O}{\|}}{C}-\langle\!\!\langle\bigcirc\rangle\!\!\rangle-O\underset{\underset{O}{\|}}{C}-\langle\!\!\langle\bigcirc\rangle\!\!\rangle-O(CH_2)_nO-\langle\!\!\langle\bigcirc\rangle\!\!\rangle-\underset{\underset{O}{\|}}{C}-$$

$$\mathbf{C_5C_n}\ (n=5\text{--}12)$$

* Author for correspondence.

The aliphatic chain connected to the mesogenic cores by two ester linking groups contains five methylene groups, while the other aliphatic chain, linked to the mesogenic cores by two ether groups contains a variable number n of methylene groups with n ranging from 5 to 12. These polyesters were designated as C_5C_n where 5 and n indicate the number of methylene groups in the two polymethylene spacers. All polyesters C_5C_n present a smectic mesophase, while a nematic mesophase is also shown by polymer samples with relatively short alkylene segments ($n = 5$–8, 10). The nematic to isotropic and smectic to nematic or to isotropic phase transition behaviour follows distinct trends. While the stability of the nematic mesophases decreases with increasing n, with a typical odd–even oscillation in which members with even n possess higher temperatures than adjacent members with odd n, the stability of the smectic mesophases increases with increasing n with an opposite trend in the odd–even alternation. The nature of the smectic mesophases was investigated by X-ray diffraction analysis on powder specimens. In all cases, the diffraction patterns were consistent with a smectic mesophase of low order. A remarkable odd–even alternation of the smectic layer thickness is exhibited, with the larger values in even members. However, with unoriented samples, it was impossible to categorize the disordered smectic in terms of either the orthogonal modification A or the tilted C one.

The aim of the present study is to report an X-ray examination on oriented fibres of polyesters C_5C_5, C_5C_7, C_5C_9, C_5C_{10} and C_5C_{12} that allows the assignment of a smectic C-like structure with unusual characteristics.

2.   Experimental
2.1. *Materials*

Polymers C_5C_n were prepared by a polycondensation reaction from 1,5-penta-methylene di-4-hydroxybenzoate and the corresponding 4,4′-alkylenedioxydibenzoic acid chloride with benzyltributylammonium bromide as the phase transfer catalyst. Number average molecular weights ($\bar{M}_n$) between $12\,400\,\mathrm{g\,mol^{-1}}$ and $30\,400\,\mathrm{g\,mol^{-1}}$ with first polydispersity index ($\bar{M}_w/\bar{M}_n$) between 1·7 and 2·0 were obtained. The phase transition parameters, taken from the relevant DSC heating and cooling curves are listed in table 1.

2.2. *Techniques*

Oriented smectic phases were produced by drawing fibres from the mesophase, at a temperature 20 K lower than the smectic to isotropic or smectic to nematic transition temperature, with a pair of tweezers at a speed of about $0·1\,\mathrm{m\,s^{-1}}$ and cooling them in air at room temperature. Accordingly, the average chain axis of the polymer corresponds to the fibre axis. X-ray measurements were performed by using a Rigaku DENKI RV300 rotating anode generator equipped with a pin-hole flat camera. Ni-filtered Cu K_α ($\lambda = 1·54\,\text{Å}$) radiation was used. The distance between samples and film was 74·5 mm. The optical density of the X-ray diffraction photographs was measured with a microdensitometer. From these data, the intensity (I) along some specified directions on the film was easily obtained. The values of the integrated intensity of the different reflections were obtained from the diffraction patterns by performing microdensitometer scans along straight lines at different angles with respect to the equatorial direction, in order to obtain the intensity profile for a set of azimuthal angles β. The numerical integration of this set of intensity profiles gave the integrated intensity of the reflections.

Table 1. Physico-chemical properties of liquid crystalline polyesters C_5C_5, C_5C_7, C_5C_9, C_5C_{10} and C_5C_{12}. Phase transition temperatures (K) and entropy changes ($J\,mol^{-1}\,K^{-1}$) in parentheses.

Sample	$\bar{M}_n/g\,mol^{-1}$†	$\bar{M}_w/\bar{M}_n$†	Phase transition‡
C_5C_5	12400	1·72	g 329 C 378 S 413 (5·3) N 420 (0·2) I I 415 (0·2) N 407 (5·4) S 353 C 326 g
C_5C_7	23400	1·96	g 306 S 424 (7·8) I I 412 (0·7) N 404 (7·2) S 300 g
C_5C_9	15800	1·97	g 297 S 440 (18·4) I I 417 (19·4) S 294 g
C_5C_{10}	30400	1·79	g 296 S 428 (8·0) N 437 (4·8) I I 430 (4·9) N 411 (8·3) S 290 g
C_5C_{12}	17000	1·76	g 292 S 436 (21.1) I I 422 (21.8) S 290 g

† By SEC, in chloroform at 30°C.
‡ g = glassy, C = crystalline, S = disordered smectic, N = nematic, I = isotropic; first line of data obtained on heating, second line on cooling (scanning rate $10\,K\,min^{-1}$).

Depending on the intensity of the diffraction peaks, different exposure times of the film were required, varying from a minimum of 10 min for the strongest peak to a maximum of ten hours for the weakest, with generator voltage 40 kV and current 200 mA. The determination of the intensity ratios of the strongest to the weakest peaks was achieved by repeating the measurements on the same sample for different exposure times under the same experimental conditions.

3. Results and discussion
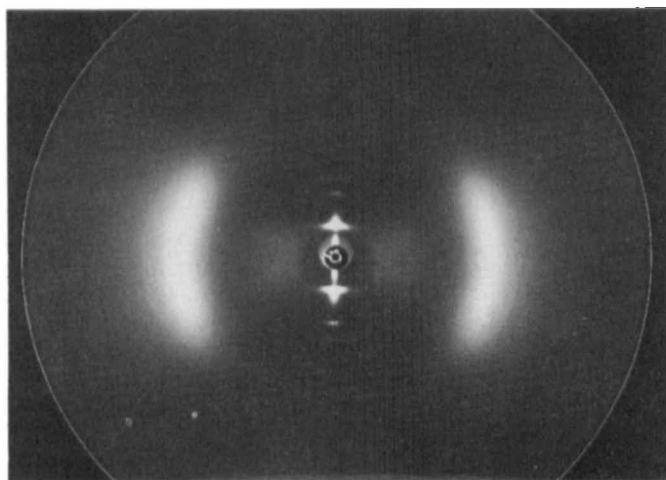### 3.1. *Description of the X-ray diffraction patterns*
In figures 1 (*a*)–(*c*), the X-ray diffraction patterns of the oriented smectic mesophases of polyesters C_5C_5, C_5C_{10} and C_5C_{12}, respectively, are reported, as typical examples while in figure 1(*d*) is schematically represented the intensity contour map of sample C_5C_{10}. The anisotropy shown in the X-ray pattern of oriented samples clearly demonstrates that a high degree of molecular orientation can be achieved by drawing fibres from the mesophases. All the diffraction patterns consist of small angle sharp reflections and wide angle broad haloes, in agreement with the presence of a disordered lamellar structure. The relevant X-ray data are collected in table 2. In the wide angle region, four diffuse crescents, relatively well-resolved for samples C_5C_5 and C_5C_7, but strongly overlapping for the other three samples, are observed. This pattern is characteristic of the unstructured liquid-like nature of the layers. The diffuse crescents are roughly equidistant from the origin and form pairs on a straight line making an angle β with respect to the equatorial line. In figure 2 the microdensitometer profile of the intensity distribution function $I(\beta)$ as a function of the azimuthal angle β is reported for sample C_5C_5 as a typical example. The tilt angle β is estimated as the angle corresponding to the maximum intensity $I(\beta)$. The amplitude of the tilt angle ranges from $\beta = 38°$ for sample C_5C_5 to $\beta = 18°$ for sample C_5C_{12} and seems to decrease with increasing n as shown in table 2. As the broad reflections are likely to result mainly from

the lateral packing of the rigid mesogenic groups, they appear to be tilted by the angle β with respect to the director of the layer planes.

The small angle Bragg reflections of all the samples are located on the meridional line, thus indicating that the fibre axis, and hence the polymer chain axis, is perpendicular to the smectic layers. All the samples exhibit a very strong low angle peak, whose periodicity ranges from $d = 14.9\,\text{Å}$ for sample C_5C_5 to $d = 21.1\,\text{Å}$ for sample C_5C_{12} (see table 2). In addition, the diffraction patterns of polyesters C_5C_7, C_5C_9, C_5C_{10} and C_5C_{12} show respectively two, two, three and four further reflections. As a typical example, in figure 3 is reported the microdensitometer profile of the intensity distribution function $I(2\theta)$ as a function of the diffraction angle 2θ for sample C_5C_{10}. Comparing the values of the lattice spacings, it appears that for each sample only a few reflections are correlated with the apparent first order. However, if we

(*a*)

(*b*)

(c)

(d)
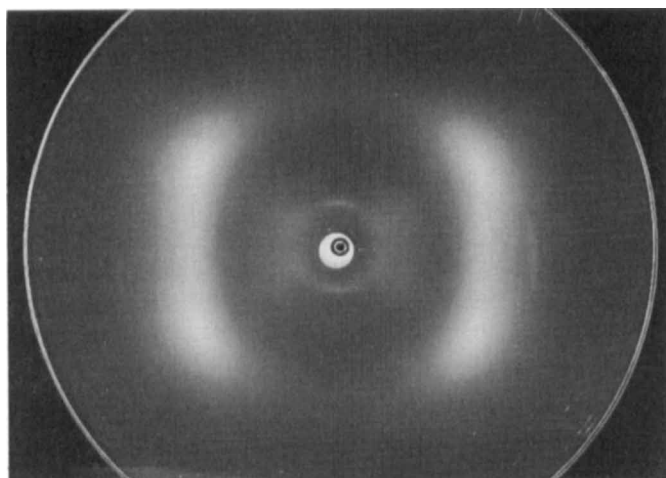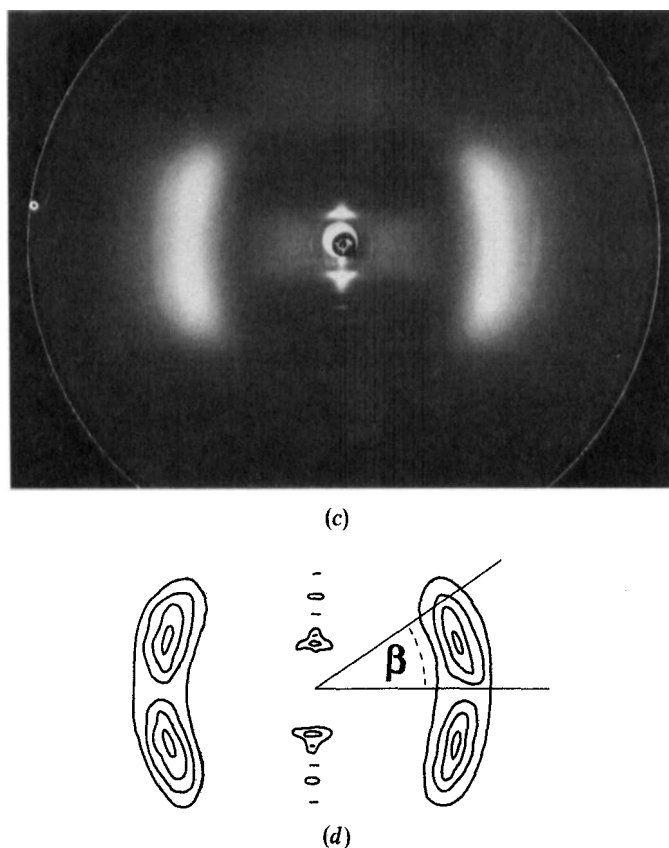
Figure 1. X-ray diffraction patterns of the fibrous smectic mesophase of polymers (a) C_5C_5, (b) C_5C_{10}, (c) C_5C_{12} and a schematic representation of the intensity contour map of polymer (d) C_5C_{10}. The fibre axis is in the vertical direction.

Table 2. X-ray diffraction data for the liquid crystalline polyesters C_5C_n determined from fibre patterns.

Sample	$\beta/°$	hkl	$d_{obs}/\text{Å}$
C_5C_5	38 ± 3	002	14·9
C_5C_7	25 ± 3	002	16·9
		003	11·4
		004	8·5
C_5C_9	25 ± 4	002	18·2
		003	12·2
		004	9·2
C_5C_{10}	18 ± 4	002	20·0
		003	13·4
		004	10·0
		005	8·0
C_5C_{12}	18 ± 3	002	21·1
		003	14·1
		004	10·5
		005	8·4
		006	7·0

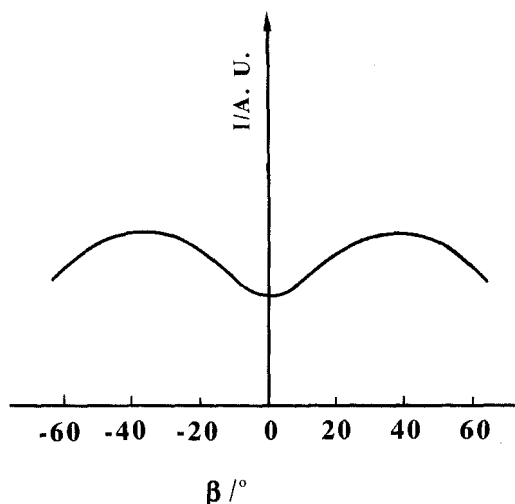Figure 2.   Intensity distribution $I(\beta)$ of polymer C_5C_5 as a function of the azimuthal angle β at a diffraction angle $2\theta = 20°$.

suppose that the observed first order reflection is indeed the true second order of a ghost first order reflection, then all the signals can be attributed to the series of $00l$ layer reflections. So we can conclude that some structural regularity interferes with the appearance of the 001 layer reflection or, in other words, the first order is extinguished. From now on, let us consider the first small angle reflection observed as the 002 reflection and the others as consequent.

The intensity profile of the small angle peaks along the meridional line of the latter four samples displays other peculiar characteristics. The 002 reflection dominates the others, with an intensity at least 20 times higher. Indeed, it is the only reflection evidenced by the measurements on powder specimens [1, 2]. In addition, while the intensity of the even order reflections for samples C_5C_{10} and C_5C_{12} decreases, the intensity of the odd order reflections increases slightly with increasing the reflection order (see figure 3), thus producing an intensity alternation with the reflection order.

The main question arising from the above results concerns the chain conformation and arrangement in the smectic layers. The most likely chain assembly, consistent with the above evidence, is illustrated for sample C_5C_{10} in figure 4. This model is similar to the model proposed in [3, 4] for the extended-chain structure of PB-7 and BB-5 polyesters in the smectic C phase. While the aliphatic chains lie along the average chain axis, the two mesogenic groups in the repeating unit are tilted to the layer normal by opposite angles. This type of smectic mesophase can be classified as unconventional smectic C. The layer spacings estimated for this structural arrangement, under the assumption that both the flexible spacers are in the fully extended conformation and lie along the molecular axis perpendicular to the smectic layers, for the various polymer samples, are as follows: C_5C_5 $d_{calc} = 32·2$ Å, C_5C_7 $d_{calc} = 37·6$ Å, C_5C_9 $d_{calc} = 40·0$ Å, C_5C_{10} $d_{calc} = 42·4$ Å, C_5C_{12} $d_{calc} = 44·8$ Å. These spacing values are more than twice as big as the 002 reflections observed (see table 2). According to the diffuse cone model [5], a difference between the observed and the calculated values is due to the orientational disorder which should produce an average tilt angle of 19° of the molecules against the layer normal. The new layer spacings calculated by applying
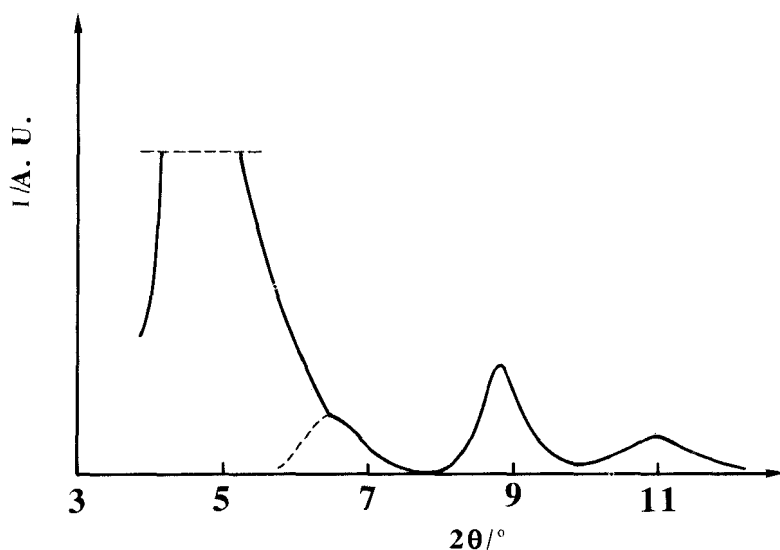
Figure 3. Intensity distribution $I(2\theta)$ of polymer C_5C_{10} as a function of the diffraction angle 2θ.

this to the present polymeric system, are as follows: C_5C_5 $d_{calc} = 30\cdot4$ Å, C_5C_7 $d_{calc} = 35\cdot6$ Å, C_5C_9 $d_{calc} = 37\cdot8$ Å, C_5C_{10} $d_{calc} = 40\cdot0$ Å, C_5C_{12} $d_{calc} = 42\cdot4$ Å and, being nearly twice the values of the 002 reflections observed, agree reasonably well with the experimental data. However, the $d/2$ sub-periodicity of the electron density distribution, responsible for extinguishing the first order reflection, cannot be recognized within the polymer repeating unit. In fact, the two flexible spacers are different as far as both the nature of the linking groups and the length of the aliphatic chains are concerned. The latter difference is at a minimum for samples C_5C_5 and C_5C_7 and increases progressively with the number n of methylene groups. In addition, the orientation of the two mesogenic groups in the repeating unit is opposite.

Another important question to be investigated is the nature of the weak reflections in the X-ray pattern of samples C_5C_7, C_5C_9, C_5C_{10} and C_5C_{12}. To clarify these points a structural model, which fits the experimentally observed data, has been proposed.

3.2. *Model for the interpretation of the X-ray diffraction patterns*

The presence of many orders of reflection in the X-ray diffraction pattern means that the projection of the electron density profile along the normal to the layers cannot be described by the ideal model of a single sinusoidal modulation [6]. However, due to the great difference in the intensity values between the strongest reflection and the other orders we should expect a density distribution only slightly different from the sinusoidal modulation corresponding to the dominant reflection. In order to obtain more information on the electron density profile, the integrated intensities of the different Bragg reflections were measured and the results, after correction both for the polarization and Lorentz factors [7], are reported in table 3. Due to the weakness of the higher order reflections and to the two dimensional nature of the reflection peaks, the integrated intensity values are not very accurate, with a roughly 20 per cent estimated error. Since we do not measure absolute scattering intensities, the results are presented as ratios $I(00l)/I(002)$ of the integrated intensity of the $00l$ reflection to the integrated intensity of the 002 reflection. Since the Bragg spots are resolution limited, we are

Figure 4.   Schematic representation of the extended-chain structure of the polymers C_5C_n.

Table 3.   Experimental and calculated (for the chain structural arrangement reported in figure 5(b)) normalized diffraction intensity of the 00*l* reflections of polyesters C_5C_7, C_5C_9, C_5C_{10} and C_5C_{12} from the fibre patterns, together with the relevant shift value D between two adjacent chains.

Sample	hkl	$[I(00l)/I(002)]_{exp}$	$D/\%$	$[I(00l)/I(002)]_{calc}$
C_5C_7	001	0·000	51·5	0·001
	002	1·000		1·000
	003	0·004		0·001
	004	0·070		0·075
C_5C_9	001	0·000	52·0	0·001
	002	1·000		1·000
	003	0·003		0·003
	004	0·032		0·030
C_5C_{10}	001	0·000	52·2	0·001
	002	1·000		1·000
	003	0·004		0·005
	004	0·027		0·026
	005	0·025		0·023
C_5C_{12}	001	0·000	52·0	0·001
	002	1·000		1·000
	003	0·006		0·006
	004	0·022		0·022
	005	0·020		0·021

interested only in the integrated intensity of the reflections and not in their shape. Once the integrated intensity reflection ratios have been determined, the electron density profile can be obtained in principle by inverse Fourier transform [7, 8]. However, in our case the phase problem connected to the nature of the structure factor is particularly complex and cannot be solved univocally with the theoretical approaches available in the literature [9]. Consequently, the problem of determining the electron density distribution is tackled directly. A reasonable electron density model is formulated and its reliability is verified a posteriori by comparing the intensity ratios

$I(00i)/I(002)$, calculated by the Fourier transform of the density model, with the corresponding experimental data. The electronic density distribution of the repeating unit is estimated by localizing the atomic electrons at fixed positions along the chain, at distances corresponding to standard atomic bond lengths [9], and the repeating unit is divided into segments where the number of electrons per unit length can be roughly considered uniform. These segments have been identified as the benzene rings, the aliphatic chains and the ether and ester linking groups. The electron density in each of these segments is calculated as the ratio of the total number of electrons to the length of the group. The electron density distribution perpendicular to the smectic layers can be obtained from the electron density model of the repeating unit once the side-by-side association of the chains has been assumed.

Concerning the possible side-by-side arrangement of the polymer chains, we consider at first the one obtained from the side-by-side association of corresponding mesogenic groups from the different chains. The resulting chain structural arrangement is shown in figure 5 (a) where the unit cell is also evidenced. The electron density profile, normal to the smectic planes, is obtained by the projection of the electron distribution of the chain structural arrangement in figure 5 (a) along the director. This is only a rough model of the actual distribution, since the statistical fluctuations of the chains along the director are not taken into account. The Fourier transform of the continuous one dimensional periodic electron density distribution $\rho(z)$ gives the structure factor $F(00l)$ of the $00l$ reflections according to equation (1)

$$F(00l) = \int_0^d \rho(z) \exp(2\pi i l z/d) \, dz, \tag{1}$$

where d is the length of the repeating unit. Indeed, in equation (1), $\rho(z)$ is the bond atomic electron density which coincides with the free atomic electron density when the scattering factor of each atom assumes its limiting value for zero scattering angle 2θ. Because the reflections considered in the present analysis correspond to small scattering angles ($\sin\theta/\lambda < 0.06$), the atomic scattering factors can be considered equal to their limiting value for zero scattering angle 2θ, within an accuracy of a few per cent.
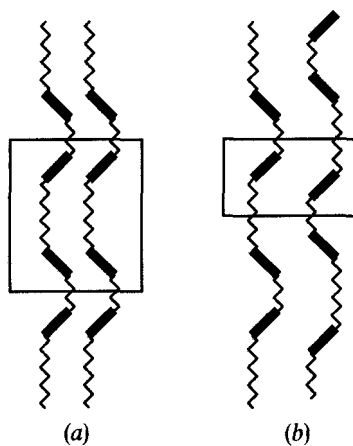

(a)   *(b)*

Figure 5. Schematic representations—see text—of models of the chain structural arrangement in the smectic mesophases of the polymers C_5C_n.

As the repeating unit is divided into N segments where the electron density takes a constant value, equation (1) assumes the following form:

$$F(00l) = \sum_{j=1}^{N} \rho_j d_j \exp(2\pi i l z'_j/d) \frac{\sin(\pi l \delta_j/d)}{(\pi l \delta_j/d)}, \quad (2)$$

where d is the layer thickness, that coincides with the length of the repeating unit only when it is not tilted to the layer normal, $\delta_j = z_{j+1} - z_j$ and $z'_j = (z_{j+1} + z_j)/2$ are respectively the width and the centre of the jth segment and ρ_j is the jth segment electron density value. The product $\rho_j \delta_j$ gives the total number of electrons n_j in the jth segment. The intensity of the reflection is proportional to the square of the structure factor

$$I(00l) \propto |F(00l)|^2. \quad (3)$$

The effect of the atomic vibrations can be accounted for by multiplying the intensities from equation (3) by the square of the Debye–Waller factor, $\exp(-l^2 B/2d^2)$, where B is the temperature factor which is related to the mean square displacement of the atoms in the direction normal to the reflecting planes. The temperature factors B have been estimated following the procedure outlined in [4, 10]. The 00l reflection intensity distribution for the chain arrangement in figure 5(a) has been determined for all the polymer samples and the main features are as follows: (i) the intensity of the 001 reflection is always greater than zero and varies from $10 (C_5C_5)$ to $50 (C_5C_{12})$ per cent of the intensity of the corresponding 002 reflection; (ii) the intensity ratio of the 001 to the 003 reflections is greater than or at least equal to 1; (iii) the intensity decay of the even 00l reflections is different from that experimentally observed. Furthermore, for samples C_5C_{10} and C_5C_{12}, the experimentally observed increase of the intensity with the order l of the odd 00l reflections is not obtained. This evidence indicates that the chain arrangement model depicted in figure 5(a) is not consistent with the experimental data. The reason lies in the form of the electron density distribution which does not show the necessary $d/2$ sub-periodicity responsible for extinguishing the first order reflection. In fact, only a very high degree of perfection of the sub-periodicity could produce the observed diffraction patterns. A structural arrangement giving rise to a $d/2$ periodic regularity starting with a chain repeating unit which does not possess any $d/2$ sub-periodicity is shown in figure 5(b). This structural arrangement originates from the side-by-side association of two chains where the corresponding repeating units are shifted by half their length d. The electron density distribution along the director is determined by projecting along z the electron density of the chain structural arrangement shown in figure 5(b). A parameter D was introduced, defined as $D = h/d \cdot 100$ where h is the distance along the z axis between the representative points of the repeat units of two adjacent polymer chains, and d is the (001) reflection layer thickness. Accordingly, D represents the value of the shift between the two adjacent chains, and the Fourier transform of the electron density is performed by varying D until the best fit of the intensity profile to the experimental data is reached. The results of the best fit obtained for the structural model of figure 5(b) are summarized in table 3 where, for each sample, the experimental and calculated normalized diffraction intensity data are reported together with the corresponding values of the shift D. If the shift between the two chains is exactly $d/2$, the periodicity of the structure reduces to half the length of the repeating unit and the calculated diffraction patterns shows only peaks corresponding to even orders 00l of the reflection, while no trace of 00l odd reflections appears. A shift value, even slightly different from $d/2$, causes the unit cell to

lose its $d/2$ periodicity so that the structure becomes strictly periodic with period d even if it keeps substantially a $d/2$ periodic character. As a consequence, the occurrence of low angle $00l$ odd reflections is observed in the calculated diffraction pattern, with intensity values depending on the extent of the shift. In addition, the experimentally observed intensity increase of the $00l$ odd reflections, with increasing order l, is reproduced. In conclusion, the intensity values so calculated , for the chain arrangement sketched in figure 5 (*b*), are in good agreement with the experimental data.

4. Conclusion

An X-ray investigation of the oriented smectic mesophase for polyesters C_5C_5, C_5C_7, C_5C_9, C_5C_{10} and C_5C_{12} is reported. The X-ray diffraction patterns are very similar for all the samples and are constituted by one or more inner reflections, lying on the meridional line, attributed to the regular piling of the smectic layers and by two broad outer haloes split into two intense portions symmetrically placed above and below the equatorial line, attributed to the rigid mesogenic groups. This evidence indicates that the mesogenic groups are tilted with respect to the layer normal while the average chain axis lines perpendicular to the layer planes. Accordingly, the smectic mesophase exhibited by the polyesters can be classified as unconventional smectic C.

The analysis of the intensity profile of the reflections from the smectic layers indicates that the 001 layer reflection is extinguished, although a structural regularity responsible for the extinction cannot be detected inside the chain repeating unit. In addition, a non-monotonic decrease of the intensity with increasing order of the reflections is observed.

To account for the above peculiarities of the X-ray diffraction spectra, we have proposed a chain structural arrangement in which two adjacent chains are shifted by about half the length of the repeating unit. The Fourier transform of the projection of the electron density profile along the normal to the layer for such a structural arrangement has been performed and the resulting calculated intensity distribution for all the polymer samples is in good agreement with the experimental results.

References

[1] CHIELLINI, E., GALLI, G., BING, Y., FRANCESCANGELI, O., MELONE, S., ANGELONI, A. S., LAUS, M., and CARETTI, D., 1992, *Molec. Crystals liq. Crystals*, **215**, 279.
[2] CHIELLINI, E., GALLI, G., LAUS, M., ANGELONI, A. S., FRANCESCANGELI, O., and BING, Y., 1992, *J. Mater. Chem.*, **2**, 449.
[3] KRIGBAUM, W. R., WATANABE, J., and ISHIKAWA, T., 1983, *Macromolecules*, **16**, 1271.
[4] WATANABE, J., and HAYASHI, M., 1989, *Macromolecules*, **22**, 4083.
[5] DE VRIES, A., EKACHAI, A., and SPIELBERG, N., 1979, *Molec. Crystals liq. Crystals*, **49**, 143.
[6] DE GENNES, P. G., 1974, *The Physics of Liquid Crystals* (Clarendon Press), p. 273.
[7] HOSEMANN, R., and BAGCHI, S. N., 1962, *Direct Analysis of Diffraction by Matter* (North Holland Publishing Company).
[8] KAKUDO, M., and KASAI, N., 1972, *X-Ray Diffraction by Polymers* (Elsevier).
[9] DAVIDSON, P. LEVELUT, A. M., ACHARD, M. F., and HARDOUIN, F., 1989, *Liq. Crystals*, **4**, 561.
[10] LEADBETTER, A. J., 1979, *The Molecular Physics of Liquid Crystals*, edited by G. R. Luckhurst and G. W. Gray (Academic Press), Chap. 13.